molecules

MDPI

Article

Synthesis, Photophysics and Tunable Reverse Saturable Absorption of Bis-Tridentate Iridium(III) Complexes via Modification on Diimine Ligand

Guochang Li, Zhao Jiang, Meng Tang, Xiaoli Jiang, Houfu Tu, Senqiang Zhu *, Rui Liu * and Hongjun Zhu

School of Chemistry and Molecular Engineering, Nanjing Tech University, Nanjing 211816, China
* Correspondence: zhusenqiang1993@njtech.edu.cn (S.Z.); rui.liu@njtech.edu.cn (R.L.)

Abstract: Five novel bis-tridentate Ir(III) complexes (**Ir-1**–**Ir-5**) incorporating versatile NˆNˆC ligands and a NˆCˆN ligand (1,3-di(2-pyridyl)-4,6-dimethylbenzene) were synthesized. With the combination of experimental and theoretical methods, their steady and transient state characteristics were researched scientifically. The UV-visible absorption spectra show that the broadband charge transfer absorbance of those bis-tridentate Ir(III) complexes can reach 550 nm, all of these complexes reveal the long-lasting phosphorescent emission. Because the excited-state absorption is more powerful than the ground-state absorption, a sturdy reverse saturable absorption (RSA) process can ensue in the visible and near-infrared regions when the complexes are exposed to a 532 nm laser. Therefore, the optical power limiting (OPL) effect follows the trend: **Ir-5** > **Ir-4** ≈ **Ir-3** > **Ir-2** > **Ir-1**. Generally speaking, the expansion of π-conjugation and the introduction of electron donating/withdrawing groups on the NˆNˆC ligand could effectively elevate the OPL effect. Therefore, these octahedral bis-tridentate Ir(III) complexes might be exploited as potential OPL materials.

Keywords: bis-tridentate Ir(III) complex; photophysical property; reverse saturable absorption; optical limiting material

check for updates

Citation: Li, G.; Jiang, Z.; Tang, M.; Jiang, X.; Tu, H.; Zhu, S.; Liu, R.; Zhu, H. Synthesis, Photophysics and Tunable Reverse Saturable Absorption of Bis-Tridentate Iridium(III) Complexes via Modification on Diimine Ligand. *Molecules* **2023**, *28*, 566. https://doi.org/10.3390/molecules28020566

Academic Editors: You Wang, Jiyong Yao, Zheng Xie and Yan Feng

Received: 26 November 2022
Revised: 25 December 2022
Accepted: 2 January 2023
Published: 5 January 2023

Copyright: © 2023 by the authors. Licensee MDPI, Basel, Switzerland. This article is an open access article distributed under the terms and conditions of the Creative Commons Attribution (CC BY) license (https://creativecommons.org/licenses/by/4.0/).

1. Introduction

Ir(III) complexes are extensively used as organic light-emitting devices (OLEDs) [1–4], low-power up conversions [5,6], organic light-emitting electrochemical transistors [7], photocatalysts [8–10], and nonlinear optics [11–13]. This application inherently relies on their comprehensive photochemical and photophysical characteristics. The Ir(III) ion's robust spin-orbit coupling effect leads to high-efficiency intersystem crossing (ISC) and a significant quantum yield of the triplet state [14]. Additionally, their photophysical characteristics may be tuned by structurally modifying the ligands in order to satisfy the necessities for various functions.

Organometallic Ir(III) complexes are thought to be potential nonlinear optical materials due to their extensive ground-state absorption (GSA) and strong excited-state absorption (ESA). Because the ESA is more powerful than the GSA, the reverse saturable absorption (RSA—the absorptivity of these complexes would heighten as the incoming light intensity increased) process occurs, which is one of the nonlinear absorption (NLA) behaviors [15–18]. In this respect, it has been reported that numerous Ir(III) complexes can be used as effective RSA materials [19,20]. The charge transfer (CT) driven by the D-π interaction between the metal and the chelating ligand is also of benefit to the NLA response [14]. Traditional Ir(III) complexes involving three bidentate ligands have been extensively researched in the field of optical power limiting (OPL) performance, due to their extreme synthetic versatility and tunable triplet excited properties [20,21]. Although the interest in tris-bidentate Ir(III) complexes is certainly increasing, these complexes suffer from unsatisfactory stability, causing by the poor resistance of bidentate chelate for undergoing metal–ligand dissociation [22].

Therefore, bis-tridentate Ir(III) complexes with robust architecture are thus considered to be promising OPL materials.

Since bis-tridentate Ir(III) complexes were first reported by Williams et al. [23], most of the reported works are focused on the field of OLEDs [24,25]. There is far less investigation of bis-tridentate ligands Ir(III) complexes, though interest in OPL materials is certainly increasing. Sun et al. firstly accounted for a variety of bis-cyclometalated Ir (III) complexes, and systematically investigated their NLA properties [21]. Because of the strong σ-donating ability, 2,6-diphenylpyridine (dppy) and its ramifications were selected as the bis-cyclometalating ligand(CˆNˆC), which endow these Ir(III) complexes with a pronounced bathochromic shift of the charge transfer (^{1}CT)/$^1\pi,\pi^*$ bands to 400−600 nm. To evaluate the feasibility of those complexes as OPL materials, our group further investigated the impact of expanded π-conjugation and replaced substituents on their RSA characteristics [20]. Realizing that the modification of tridentate chelate would certainly influence the RSA properties, the development of those Ir(III) complexes to obtain satisfactory OPL materials remains challenging.

In this work, organometallic Ir(III) complexes bearing NˆNˆC ligand and NˆCˆN ligand (1,3-di(2-pyridyl)-4,6-dimethylbenzene) were devised and synthesized (Chart 1). To avoid the bidentate NˆC coordination, a pair of substituents (−CH_3) were simultaneously inserted at the 4th and 6th locations of the central benzene ring at the same time. Phenanthroline and fluorene were employed as a building block to expand the π-conjugation of NˆNˆC ligand (**Ir-2** and **Ir-3**), which is due to their high structural rigidities and good charge transporting abilities. Naphthalimide and carbazole units are introduced to further explore the influence of electron donating/withdrawing groups (**Ir-4** and **Ir-5**). A suite of spectroscopic methods and theoretical models were used to investigate their physicochemical characteristics systematically. These directed Ir(III) complexes have adjustable ground-state and triplet excited-state properties, which satisfied the OPL requirements. This work gains insight into the RSA property–structure relationship among these bis-tridentate Ir(III) complexes and serves as a modified version for certain nonlinear optical absorbers [26–28].

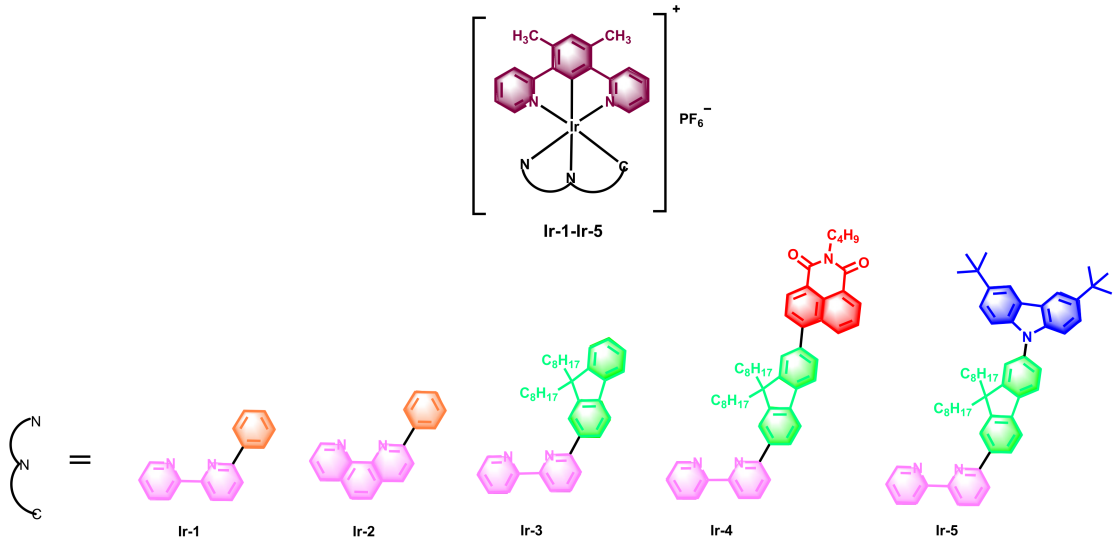


Chart 1. The molecular structures to complexes **Ir-1**–**Ir-5**.

2. Results and Discussion

2.1. Design and Synthesis

To adjust the ground and excited-state characteristics of the bis-tridentate complexes, different strategies were performed. To show the influences of enlarged π-conjugation, additional aromatic rings of the NˆNˆC ligands were inserted (**Ir-2** and **Ir-3**), while strong electron or withdrawing substituents are recommended to further satisfy the RSA properties for OPL properties. In addition, long alkyl chains were linked to both fluorene and

naphthalimide groups, which were used to avoid the intermolecular aggregation and improve the solubility of the Ir(III) complexes.

The NˆNˆC ligands were created by combining aryl halides with phenylboronic acid in the Suzuki coupling reaction and were obtained in 50–60% yield after recrystallization. A conventional two-step technique was used to accurately produce the corresponding octahedral Ir(III) complexes **Ir-1**–**Ir-5**. This two-step method is often disseminated in mild settings, with middling yields. These complexes were all air-stable and soluble in CH_2Cl_2, toluene, tetrahydrofuran (THF), *N*, *N*-dimethylformamide (DMF), and dimethyl sulphoxide (DMSO). The predicted structure of **Ir-1**–**Ir-5** was validated by ^{1}H NMR and HRMS.

2.2. Ground State UV-Vis Absorption

The UV-vis absorption spectra of five Ir(III) complexes in CH_3CN are shown in Figure 1, and Table 1 summarized the detailed photophysical data. Below 300 nm, all of these complexes exhibit significant structured absorption bands, which are attributed to the intra-ligand $^1\pi$-π^* transitions from diimine ligands. The spin-allowed charge transfer transitions, such as ^{1}MLCT (metal-to-ligand changer transfer) and ^{1}LLCT (ligand-to-ligand charger transfer), are responsible for the medium absorption regions at 350–500 nm. For **Ir-4** and **Ir-5**, above 500 nm, the absorption bands of the low energy tail can be referred to a mixed state, including spin-forbidden ^{3}MLCT/^{3}LLCT and $^3\pi$-π^* transition [29,30]. Comparing the complexes **Ir-1**, **Ir-2,** and **Ir-3**, the increase in π-conjugation on the NˆNˆC ligand resulted in a red shift in the absorption band. In contrast, the electron-withdrawing/donating substituents evoked a major effect on the energy, and the absorption bands of **Ir-4** and **Ir-5** are a more bathochromic shift in comparison to those of **Ir-3**. Additionally, compared with **Ir-4**, the absorption peak of **Ir-5** is further red-shifted, and significantly increases the absorption intensity by a concomitant increase in charge transfer contribution.

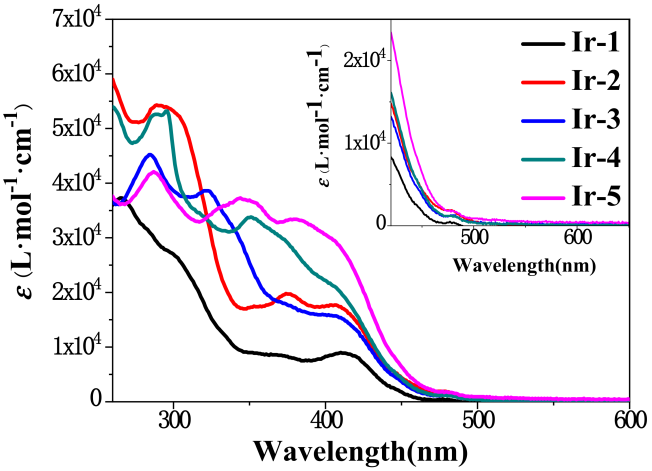


Figure 1. UV-vis absorption spectra of **Ir-1**–**Ir-5** in CH_3CN (1×10^{-5} moL/L).

Table 1. Photophysical data of complexes **Ir-1**–**Ir-5**.

Complex	λ_{abs} [a]/nm ($\varepsilon/10^4$ L·mol^{-1}·cm^{-1})	λ_{em} [b]/nm (τ_{em}/ns), Φ_{em}	$\lambda_{T1\text{-}Tn}$/nm [c] (log $\varepsilon_{T1\text{-}Tn}$, τ_{TA}/ns); Φ_T
Ir-1	273 (5.36), 348 (4.15), 409 (2.46), 468 (0.65)	594 (111); 0.34	530 (4.91, 69), 565 (5.11, 70), 0.23
Ir-2	276 (5.68), 359 (4.22), 421 (1.73), 455 (0.55)	596 (105); 0.13	560 (4.18, 86), 590 (4.57, 78), 0.26
Ir-3	276 (4.51), 362 (6.13), 430 (2.79), 480 (0.75)	609 (135); 0.29	410 (4.07, 74), 530 (4.51, 95), 605 (4.77, 56); 0.18
Ir-4	273 (6.36), 348 (5.15), 409 (2.96), 468 (0.65)	610 (241); 0.18	460 (4.91, 198), 530 (5.11, 179), 560 (5.12,94); 0.23
Ir-5	256 (5.79), 345 (4.52), 409 (2.47), 465 (0.65)	613 (341); 0.24	530 (4.09, 341), 570 (4.25, 354), 653 (4.26, 352); 0.35

[a] Electronic absorption band maxima in CH_3CN at room temperature. [b] Room temperature emission energy, lifetime, and quantum yield in CH_3CN. [c] ns TA band maxima, triplet extinction coefficients, triplet excited-state lifetimes and quantum yield in CH_3CN. The reference used was SiNc in C_6H_6 (ε_{590} = 70,000 L mol^{-1} cm^{-1}, Φ_T = 0.20).

2.3. Photoluminescence

To further comprehend the excited-state features, the emission characteristics of these Ir(III) complexes were also investigated. Figure 2 depicts the normalized emission spectra of **Ir-1**–**Ir-5**, and the corresponding parameters are reported in Table 1. All of the complexes have congruent room temperature phosphorescence, which is responsive to oxygen, and also have relatively long lifetimes. Their excitation spectra are shown in Figure S1. It is obvious that their excited-state characteristics are influenced by the modified N^N^C ligands. Although these complexes own the wide and structureless emission bands, their emission lifetimes are different. For **Ir-1**–**Ir-3,** the expansion of π-conjugation has little influence (111 ns for **Ir-1**, 105 ns for **Ir-2**, and 135 ns for **Ir-1**). However, comparing **Ir-3**–**Ir-5**, the introduction of electron-withdrawing/donating substituents prolong their lifetimes (241 ns for **Ir-4** and 341 ns for **Ir-5**), which is due to the intramolecular charge transfer. The emission properties of solvents with different polarities are further studied (Figure 2b–f). Taking **Ir-1** for example (Figure 2b), it was discovered that the low energy emission bathochromically moved to longer wavelengths in solvents with higher polarity (e.g., CH_3CN) relative to its location in the less polar solvents (e.g., THF). Considering their wide and structureless emission bands and solvatochromic effect (As show in Table 2), the emission properties of these complexes can be mainly ascribed to ^{3}MLCT/^{3}LLCT states with little $^3\pi$-π^* state [31–33].

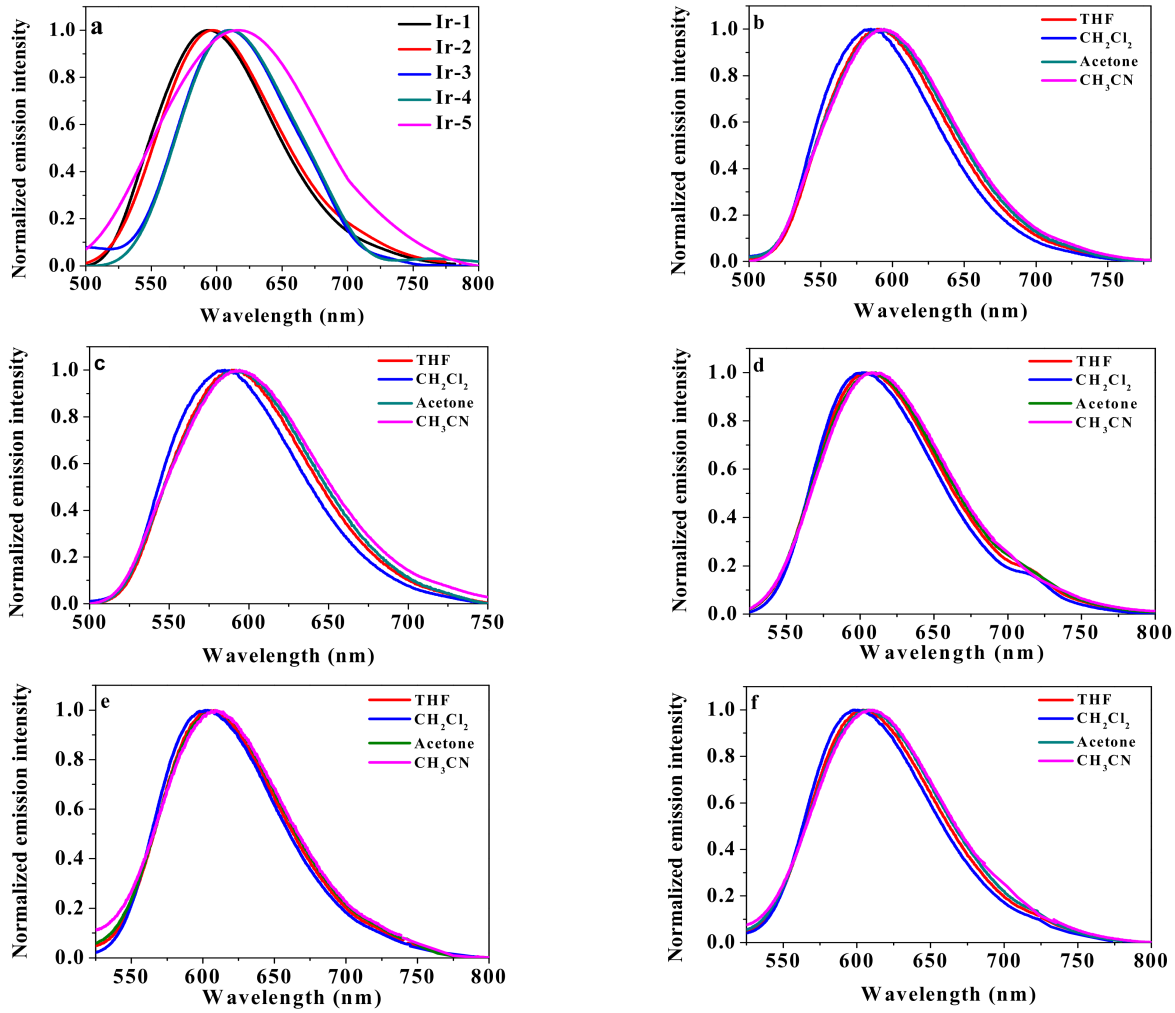


Figure 2. (**a**) Normalized emission spectra of complexes **Ir-1**–**Ir-5** in CH_3CN ($c = 1 \times 10^{-5}$ mol/L). (**b**–**f**) Normalized emission spectra of complexes **Ir-1**–**Ir-5** in different solvents.

Table 2. Emission wavelength and quantum yields of **Ir-1**–**Ir-5** in different solvents.

	λ_{em}/nm (Φ_{em})			
	THF	**CH_2Cl_2**	**Acetone**	**CH_3CN**
Ir-1	589 (0.29)	584 (0.29)	594 (0.34)	594 (0.30)
Ir-2	589 (0.19)	585 (0.13)	594 (0.13)	596 (0.17)
Ir-3	604 (0,23)	602 (0.28)	607 (0.29)	609 (0.14)
Ir-4	603 (0.18)	603 (0.24)	609 (0.18)	610 (0.12)
Ir-5	604 (0.24)	601 (0.26)	609 (0.24)	613 (0.24)

2.4. DFT Calculations

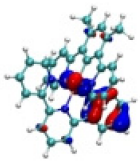
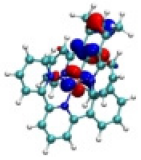
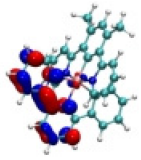
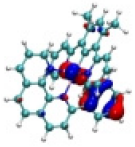
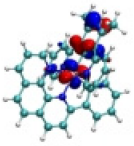
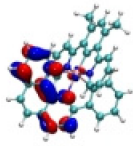
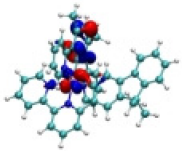
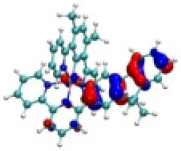
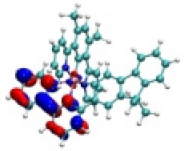
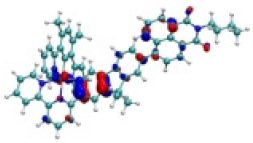
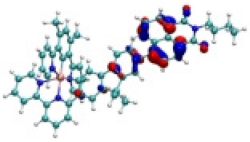
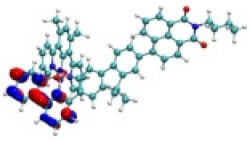
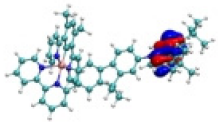
To gain a better understanding of the structure–property relationships of these complexes, the DFT calculation was carried out to acquire a thorough grasp of the underlying foundation of the aforementioned experimental findings [34,35]. Tables 3 and 4 list the excitation energies, wavelengths, oscillator strengths, associated configuration coefficients, and the major principal configuration of the lowest electronic states (highest occupied molecular orbitals (HOMOs) and lowest unoccupied molecular orbitals (LUMOs)). From Table 3, the optical transitions of S_1 and T_1 states of complexes **Ir-1**–**Ir-5** are primarily from HOMO-1→LUMO and HOMO→LUMO transitions. As shown in Table 4 and Table S1, the electron density of the HOMO of the complexes **Ir-1** and **Ir-2** is mainly distributed on NˆCˆN and the center Ir atom, and the LUMO is almost exclusively located in NˆNˆC ligand (2,2′-bipyridine of **Ir-1** and 1,10-phenanthroline of **Ir-2**). However, the electron density of the HOMO of the complex **Ir-3** is mainly distributed on the NˆNˆC ligand fluorene and Ir atom, while the LUMO is distributed the NˆNˆC ligands and the central Ir atom. In addition, the LUMO distributions of **Ir-4** and **Ir-5** share similar properties, while the electron density of the HOMO of the complexes is mainly distributed on the NˆNˆC ligand, including fluorene and terminal group (naphthalimide on **Ir-4** and carbazole on **Ir-5**). Although the orbital configurations are complicated, the major transitions of all target complexes are associated with the MLCT and LLCT transitions. Moreover, the trends of the calculated S0→S1 transition wavelengths and T1→S0 transition wavelengths for these complexes are similar to the commencement of UV-Vis absorption onset and photoluminescence.

Table 3. The calculated excitation energies (eV), wavelengths (nm), oscillator strengths, dominant contributing configurations of complexes **Ir-1**–**Ir-5**.

	State	***E*/eV**	**λ [a]/nm**	**λ [b]/nm**	***f***	**Main Configurations**	**Assignment**
Ir-1	S_1	2.3865	525	519.52	0.0001	HOMO→LUMO 98.24%	^{1}MLCT/^{1}LLCT
	T_1	2.3406	594	529.71	0	HOMO→LUMO 97.09%	^{3}MLCT/^{3}LLCT
Ir-2	S_1	2.4874	524	498.46	0.0022	HOMO→LUMO 97.53%	^{1}MLCT/^{1}LLCT
	T_1	2.3722	595	522.65	0	HOMO-1→UMO 83.18%	^{3}MLCT/^{3}LLCT
Ir-3	S_1	2.3197	527	534.49	0.0042	HOMO-1→LUMO 5.42% HOMO→LUMO 92.32%	^{1}MLCT/^{1}LLCT
	T_1	2.1172	609	585.59	0	HOMO-1→LUMO 7.33% HOMO→LUMO 88.81%	^{3}MLCT/^{3}LLCT
Ir-4	S_1	2.2264	530	556.87	0.0052	HOMO-1→LUMO 12.43% HOMO→LUMO 85.96%	^{3}MLCT/^{3}LLCT
	T_1	2.0842	610	594.89	0	HOMO-1→LUMO 29.67% HOMO→LUMO 63.21%	^{3}MLCT/^{3}LLCT
Ir-5	S_1	1.4610	538	588.64	0.0024	HOMO→ LUMO 99.57%	^{3}MLCT/^{3}LLCT
	T_1	1.4406	613	611.64	0	HOMO→ LUMO 98.17%	^{3}MLCT/^{3}LLCT

[a] Obtained from experiment. [b] Obtained from calculation.

Table 4. Frontier molecular orbitals (HOMO-1, HOMO, and LUMO) in the lowest optical transitions for complexes **Ir-1**–**Ir-5**.

	HOMO-1	HOMO	LUMO
Ir-1	 −8.06 eV	 −7.90 eV	 −4.82 eV
Ir-2	 −8.05 eV	 −7.88 eV	 −4.71 eV
Ir-3	 −7.81 eV	 −7.54 eV	 −4.70 eV
Ir-4	 −7.82 eV	 −7.33 eV	 −4.78 eV
Ir-5	 −6.87 eV	 −6.39 eV	 −4.69 eV

2.5. Transient Absorption

Nanosecond transient (TA) absorption of **Ir-1**–**Ir-5** were researched to further comprehend their triplet excited-state properties in order to determine the spectral region where RSA may happen. The nanosecond time-resolved TA spectra for complexes **Ir-1**–**Ir-5** are presented in Figure 3. Table 1 lists the lifetimes of the triplet excited states inferred from the TA decay profile and quantum yields.

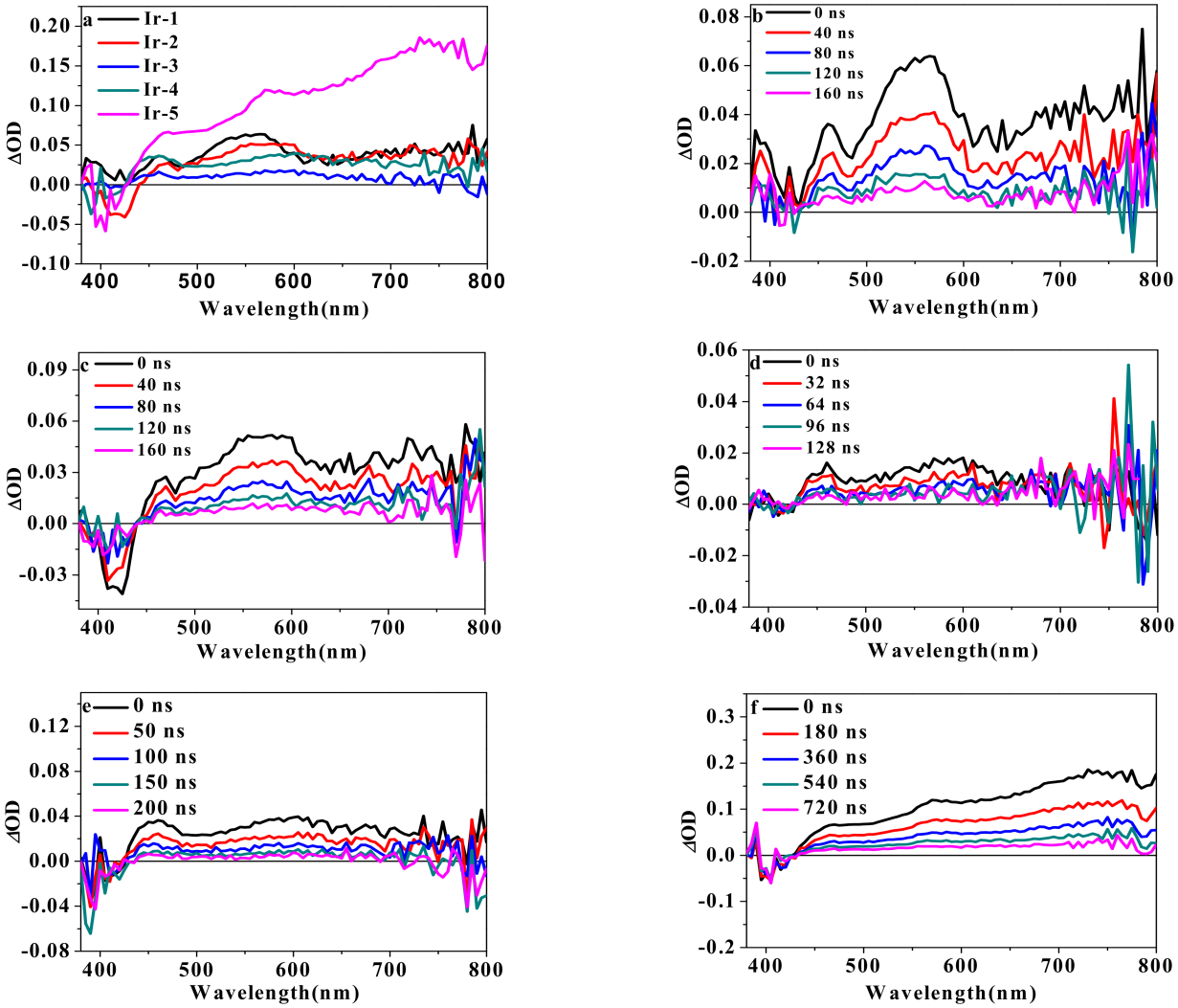


Figure 3. (**a**) Nanosecond transient difference absorption spectra of **Ir-1**–**Ir-5** in CH_3CN at zero-time decay; (**b**–**f**) time-resolved TA spectra of **Ir-1**–**Ir-5**. The spectra were all measured in CH_3CN, (λex = 355 nm, A_{355} = 0.4 in a 1 cm cuvette).

2.6. Optical Power Limiting Properties

All complexes show stronger ESA than the GSA, and the broad positive TA absorption bands (Figure 3) reveal that the RSA process would occur in these ranges. In order to assess the OPL response, the target Ir(III) complexes were irradiated with a 532 nm Nd:YAG laser [13,15,36,37]. For comparison purposes, the concentration in solution was set to 80% transmittance at 532 nm for all samples. Figure 4 demonstrated that all complexes exhibit better OPL performance than the standard OPL material (C_{60}). The output energy density reduced dramatically as the incoming laser's energy increased. As shown in Figure 4 and Table 5, the intensity of the OPL response corresponds to the trend **Ir-5** > **Ir-4** ≈ **Ir-3** > **Ir-2** > **Ir-1**. The complex **Ir-5** exhibited the best OPL ability; when the energy density of the input was raised to 1.5 cm^{-2}, the transmittance is only 20%. **Ir-5** has potential to be the broadband reverse saturable absorber in the visible–near-infrared spectral range. Compared with other bis-tridentate Ir(III) complexes, modifying electron-donating units or extending π-conjugation of the ligands is a systematic way to improve the RSA effect [20,21,38].

Based on the analysis and discussion above, Scheme 1 summarizes the RSA processes involved in the Ir(III) complexes. Under 532 nm laser excitation, the Ir(III) complexes, **Ir-1**–**Ir-5**, were excited to the S_1 state by 520 nm laser radiation. Then, Ir(III) complexes

were stimulated to a higher singlet state (S_n) or under heavy-atom-effect-induced ISC to the first triplet state (T_1). The Ir(III) complexes on the T_1 state could further absorb the photons to a higher triplet state (T_n) under the laser radiation. When the ESA is stronger than GSA, there is an effective NLA response based on the RSA process.

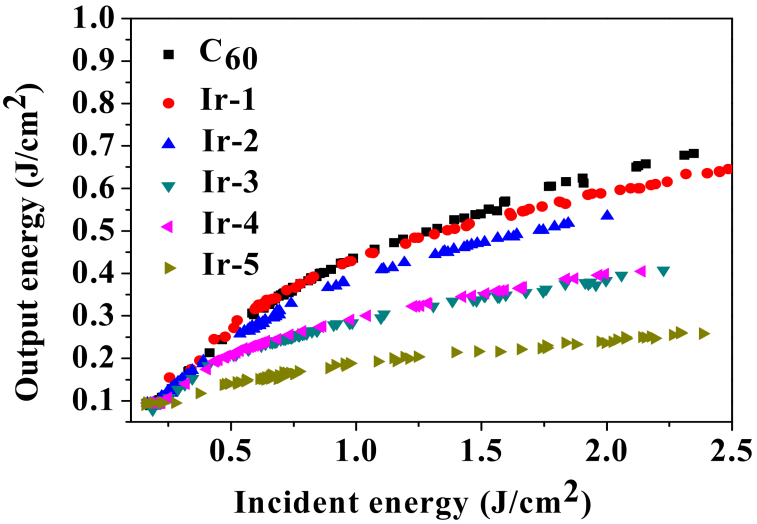
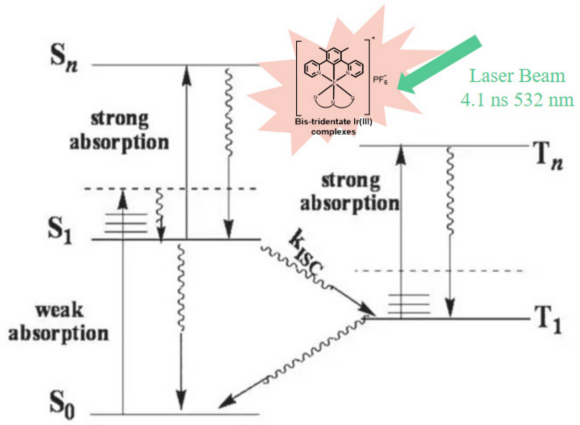


Figure 4. Output fluence vs. incident fluence for complexes **Ir-1**–**Ir-5** in CH_3CN, and C_{60} in toluene at 532 nm using a 4.1 ns laser pulse.

Table 5. The F_{50} of Ir complexes.

Complex	Ir-1	Ir-2	Ir-3	Ir-4	Ir-5
F_{50} [a] (J/cm^2)	1.23	0.95	0.52	0.55	0.22

[a] Incident energy density at a transmittance of 50%.



Scheme 1. Jablonski diagram of the RSA processes of Ir(III) complexes.

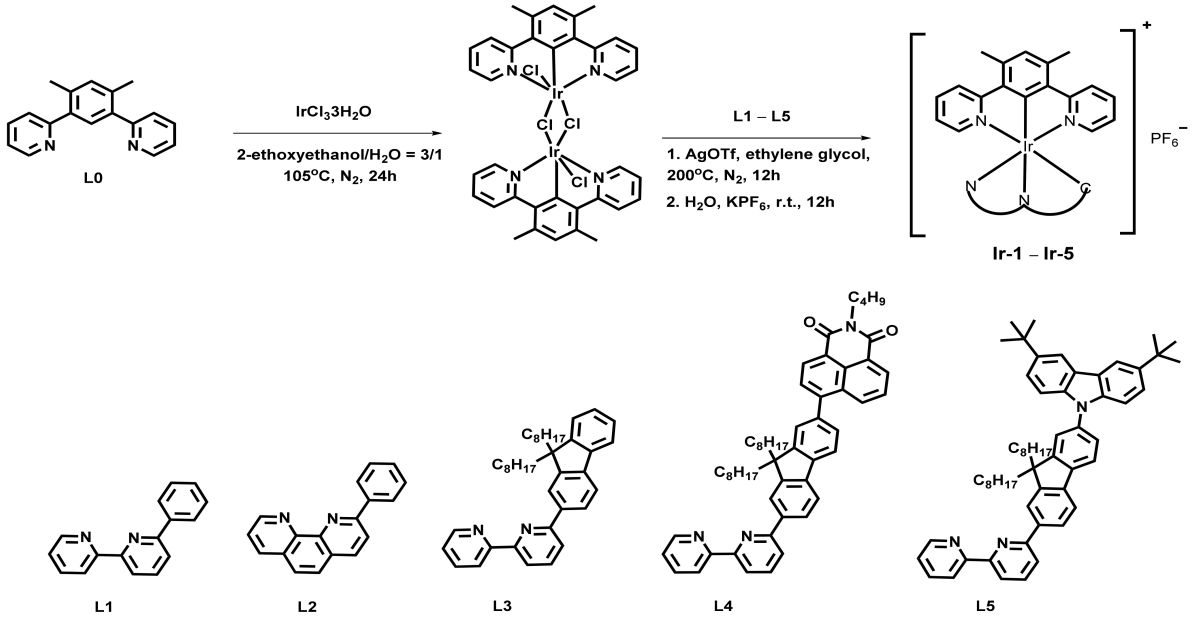
3. Experimental Section

3.1. Computational Methods

The ground electronic state frontier molecular orbitals (FMOs) of complexes **Ir-1**–**Ir-5** were simulated by density functional theory (DFT), and their excited electronic states were calculated using the time-dependent density function theory (TDDFT) method. All calculations were performed using the Gaussian 09 software package. The specific DFT method used was PBE1PBE for calculating excited electronic states. The basic sets used in all calculations were the 6–31G* set for all light atoms and the LANL2DZ set for Ir(III)

atoms. Full equilibrium geometry optimization was performed for the ground electronic states of all complexes. For consistency with experiments, acetonitrile (CH_3CN) used for experimental measurements was selected as the solvent in theoretical calculations as well.

The materials and measurements are described in depth in the supporting information. Scheme 2 outlines the synthesis of the Ir(III) complexes. **L0** was synthesized according to methods in the literature [20]. Ligands **L1**–**L5** are also presented in Scheme S1.



Scheme 2. The synthetic route to complexes **Ir-1**–**Ir-5**.

3.2. Preparation of Complexes

Preparation of the Ir chloride complexes. $IrCl_3$ (200 mg, 0.6 mmol), **L0** (0.6 mmol), ethylene glycol (30 mL), and water (10 mL) were added to a 100 mL round-bottom flask under nitrogen. The mixture was refluxed (120 °C) and stirred for 24 h. Then, using water (30 mL) to quench the reaction, the suspension was filtered. The crude product was dried at 45 °C under vacuum. Yellow solid was obtained (183 mg, yield 45%). Without further confirmation, Ir(III) chloride complexes were used in the next reaction.

Preparation of the complexes **Ir-1**–**Ir-5**. The μ-chloro-bridged dimer intermediate (523 mg, 0.5 mmol), **L1**–**L5** (1 mmol), ethylene glycol (30 mL), and $AgCF_3SO_3$ (617 mg, 2.4 mmol) were added to a 100 mL round-bottom flask under nitrogen. The mixture was refluxed with stirring for 24 h. Then, after cooling to room temperature, excess KPF_6 was added and stirred at room temperature for 3 h. The residue was taken into H_2O and extracted with dichloromethane three times. The remnant was dried over anhydrous Na_2SO_4 and concentrated. The mixture was purified by flash chromatography on a silica gel using dichloromethane and methanol (100:1, *v*/*v*) as the eluent.

Complex **Ir-1**. Yellow solid (203 mg, yield 33%). ^{1}H NMR (400 MHz, DMSO-d_6) δ 8.86–8.75 (m, 2H), 8.59 (d, *J* = 8.1 Hz, 1H), 8.39 (t, *J* = 8.1 Hz, 1H), 8.23 (d, *J* = 8.4 Hz, 2H), 8.10 (td, *J* = 8.0, 1.4 Hz, 1H), 7.91 (d, *J* = 7.3 Hz, 1H), 7.88–7.79 (m, 2H), 7.49 (dd, *J* = 10.1, 5.0 Hz, 3H), 7.40–7.33 (m, 1H), 7.18 (s, 1H), 6.98 (t, *J* = 6.5 Hz, 2H), 6.83 (t, *J* = 7.1 Hz, 1H), 6.62 (t, *J* = 7.4 Hz, 1H), 5.78 (d, *J* = 7.1 Hz, 1H), 2.92 (s, 6H). HRMS (ESI) m/z calcd for $C_{34}H_{26}IrN_4^+$ $(M)^+$ 683.1781, found 683.1785.

Complex **Ir-2**. Yellow solid (203 mg, yield 32%). ^{1}H NMR (400 MHz, DMSO-d_6) δ 8.90 (q, *J* = 8.8 Hz, 2H), 8.66 (dd, *J* = 8.3, 1.2 Hz, 1H), 8.44 (d, *J* = 8.9 Hz, 1H), 8.23 (d, *J* = 8.9 Hz, 3H), 8.04 (t, *J* = 7.5 Hz, 1H), 7.85 (dd, *J* = 5.0, 1.2 Hz, 1H), 7.82–7.75 (m, 2H), 7.61 (dd, *J* = 8.2, 5.0 Hz, 1H), 7.40–7.33 (m, 2H), 7.20 (s, 1H), 6.92–6.86 (m, 1H), 6.86–6.78 (m, 2H), 6.65 (td,

J = 7.4, 1.3 Hz, 1H), 5.92–5.84 (m, 1H), 2.93 (s, 6H). HRMS (ESI) m/z calcd for $C_{36}H_{26}IrN_4^+$ $(M)^+$ 707.1781, found 707.1787.

Complex **Ir-3**. Yellow solid (203 mg, yield 32%). ^{1}H NMR (400 MHz, DMSO-d_6) δ 8.75 (ddd, *J* = 11.1, 10.4, 5.5 Hz, 3H), 8.38 (dd, *J* = 9.5, 6.6 Hz, 1H), 8.23 (t, *J* = 9.8 Hz, 2H), 8.16 (t, *J* = 7.1 Hz, 1H), 8.08 (t, *J* = 7.6 Hz, 1H), 7.85–7.72 (m, 2H), 7.46 (dt, *J* = 10.7, 5.0 Hz, 3H), 7.38–7.33 (m, 1H), 7.31 (d, *J* = 6.9 Hz, 1H), 7.24 (s, 1H), 7.15 (d, *J* = 9.2 Hz, 1H), 7.09 (dd, *J* = 11.8, 7.2 Hz, 2H), 6.93 (t, *J* = 5.7 Hz, 2H), 6.11 (t, *J* = 2.6 Hz, 1H), 2.96 (d, *J* = 3.0 Hz, 6H), 2.09–1.78 (m, 4H), 0.82–0.11 (m, 30H). HRMS (ESI) m/z calcd for $C_{57}H_{62}IrN_4^+$ $(M)^+$ 995.4598, found 995.4597.

Complex **Ir-4**. Yellow solid (153 mg, yield 30%). ^{1}H NMR (400 MHz, DMSO-d_6) δ 8.78 (ddd, *J* = 10.4, 8.1, 2.7 Hz, 3H), 8.55–8.47 (m, 2H), 8.41 (t, *J* = 7.9 Hz, 1H), 8.26 (dd, *J* = 9.7, 6.3 Hz, 3H), 8.14–8.07 (m, 1H), 8.07–8.00 (m, 1H), 7.87–7.77 (m, 2H), 7.71 (t, *J* = 7.8 Hz, 1H), 7.63 (dd, *J* = 7.5, 1.5 Hz, 1H), 7.53–7.44 (m, 4H), 7.42–7.35 (m, 1H), 7.29 (s, 2H), 7.25 (s, 1H), 6.99–6.90 (m, 2H), 6.21 (d, *J* = 3.9 Hz, 1H), 4.05 (t, *J* = 7.2 Hz, 2H), 2.97 (s, 6H), 2.12–1.88 (m, 4H), 1.69–1.55 (m, 2H), 1.40–1.28 (m, 2H), 0.92 (t, *J* = 7.3 Hz, 3H), 0.77–0.18 (m, 30H). HRMS (ESI) m/z calcd for $C_{73}H_{75}IrN_5O_2^+$ $(M)^+$ 1246.5544, found 1246.5535.

Complex **Ir-5**. Yellow solid (203 mg, yield 32%). ^{1}H NMR (400 MHz, DMSO-d_6) δ 8.84–8.72 (m, 3H), 8.58–8.49 (m, 2H), 8.41 (t, *J* = 7.8 Hz, 1H), 8.27 (dd, *J* = 13.7, 5.9 Hz, 3H), 8.14–8.03 (m, 2H), 7.83 (dd, *J* = 17.8, 8.9 Hz, 2H), 7.73 (t, *J* = 7.8 Hz, 1H), 7.65 (d, *J* = 7.5 Hz, 1H), 7.57–7.43 (m, 4H), 7.39 (d, *J* = 5.6 Hz, 1H), 7.31 (s, 1H), 7.26 (s, 1H), 6.96 (dd, *J* = 12.0, 5.9 Hz, 2H), 6.21 (d, *J* = 3.1 Hz, 1H), 4.07 (t, *J* = 7.1 Hz, 2H), 2.98 (s, 6H), 2.51 (s, 18H), 2.10–1.91 (m, 4H), 0.87–0.22 (m, 30H). HRMS (ESI) m/z calcd for $C_{77}H_{85}IrN_5^+$ $(M)^+$ 1272.6428, found 1272.6435.

4. Conclusions

Five bis-tridentate Ir(III) complexes with different π-conjugation and terminal groups on the N^N^C ligands have been synthesized. In order to better explore the RSA properties, their photophysical characteristics have been thoroughly studied utilizing spectroscopic methods. All Ir(III) complexes exhibit intra-ligand ^{1}π-π* transitions and ^{1}LLCT/^{1}MLCT transition. The modification on the N^N^C ligands generated a bathochromic shift in the absorption band because of the increase in charge transfer contribution. The emission properties of these complexes are from the triplet excited state and can be mainly attributed to ^{3}MLCT/^{3}LLCT states with little ^{3}π-π* state. In addition, the introduction of terminal groups efficaciously prolongs the triplet excited lifetimes. Broadband triplet TA is observed in these complexes in the visible-NIR region. Considering their significantly broader GSA and higher ESA, all complexes produce a substantial NLA response, which follows the descending order **Ir-5** > **Ir-4** ≈ **Ir-3** > **Ir-2** > **Ir-1**. Therefore, these Ir(III) complexes are promising nonlinear absorber materials for the application of OPL.

Supplementary Materials: The following supporting information can be downloaded at https://www.mdpi.com/article/10.3390/molecules28020566/s1: Scheme S1: The molecular structures and synthetic route to complexes **L1-L5**; Figure S1: The excitation spectra of complexes **Ir-1**–**Ir-5** in CH_3CN; Table S1: Contribution of fragments in Ir complexes; Figure S2: ^{1}H NMR spectra (up) and mass spectrometry (down) of **Ir-1**; Figure S3: ^{1}H NMR spectra (up) and mass spectrometry (down) of **Ir-2**; Figure S4: ^{1}H NMR spectra (up) and mass spectrometry (down) of **Ir-3**; Figure S5: ^{1}H NMR spectra (up) and mass spectrometry (down) of **Ir-4**; Figure S6: ^{1}H NMR spectra (up) and mass spectrometry (down) of **Ir-5**.

Author Contributions: Conceptualization, S.Z. and R.L.; complexes production and characteristics provision, G.L., Z.J. and M.T.; formal analysis, G.L. and X.J.; computational analysis, M.T. and H.Z.; writing—review and editing, G.L., M.T., Z.J., H.T., S.Z. and R.L.; contributed reagents, materials, and analysis tools, R.L. and H.Z.; supervision, S.Z., R.L. and H.Z.; funding acquisition, S.Z., R.L. and H.Z. All authors have read and agreed to the published version of the manuscript.

Funding: The authors greatly acknowledge the Natural Science Foundation of Jiangsu Province (No. BK20220351), and the Natural Science Foundation of the Jiangsu Higher Education Institutions of China (No. 22KJB150027) for financial support.

Institutional Review Board Statement: Not applicable.

Informed Consent Statement: Not applicable.

Data Availability Statement: Not applicable.

Conflicts of Interest: The authors declare no conflict of interest.

Sample Availability: Samples of the compounds **Ir-1**–**Ir-5** are available from the authors.

References

1. Tsuboyama, A.; Iwawaki, H.; Furugori, M.; Mukaide, T.; Kamatani, J.; Igawa, S.; Moriyama, T.; Miura, S.; Takiguchi, T.; Okada, S.; et al. Homoleptic Cyclometalated Iridium Complexes with Highly Efficient Red Phosphorescence and Application to Organic Light-Emitting Diode. *J. Am. Chem. Soc.* **2003**, *125*, 12971–12979. [CrossRef] [PubMed]
2. Parker, S.T.; Slinker, J.D.; Lowry, M.S.; Cox, M.P.; Bernhard, S.; Malliaras, G.G. Improved Turn-on Times of Iridium Electroluminescent Devices by Use of Ionic Liquids. *Chem. Mater.* **2005**, *17*, 3187–3190. [CrossRef]
3. Du, B.-S.; Lin, C.-H.; Chi, Y.; Hung, J.-Y.; Chung, M.-W.; Lin, T.-Y.; Lee, G.-H.; Wong, K.-T.; Chou, P.-T.; Hung, W.-Y.; et al. Diphenyl(1-Naphthyl)Phosphine Ancillary for Assembling of Red and Orange-Emitting Ir(III) Based Phosphors; Strategic Synthesis, Photophysics, and Organic Light-Emitting Diode Fabrication. *Inorg. Chem.* **2010**, *49*, 8713–8723. [CrossRef] [PubMed]
4. Wong, W.-Y.; Zhou, G.-J.; Yu, X.-M.; Kwok, H.-S.; Lin, Z. Efficient Organic Light-Emitting Diodes Based on Sublimable Charged Iridium Phosphorescent Emitters. *Adv. Funct. Mater.* **2007**, *17*, 315–323. [CrossRef]
5. Zhao, W.; Castellano, F.N. Upconverted Emission from Pyrene and Di- *Tert* -Butylpyrene Using Ir(Ppy) $_3$ as Triplet Sensitizer. *J. Phys. Chem. A* **2006**, *110*, 11440–11445. [CrossRef]
6. Rachford, A.A.; Ziessel, R.; Bura, T.; Retailleau, P.; Castellano, F.N. Boron Dipyrromethene (Bodipy) Phosphorescence Revealed in [Ir(Ppy) $_2$ (Bpy-C≡C-Bodipy)] $^+$. *Inorg. Chem.* **2010**, *49*, 3730–3736. [CrossRef]
7. Zhou, Y.; Han, S.; Zhou, G.; Wong, W.-Y.; Roy, V.A.L. Ambipolar Organic Light-Emitting Electrochemical Transistor Based on a Heteroleptic Charged Iridium(III) Complex. *Appl. Phys. Lett.* **2013**, *102*, 083301. [CrossRef]
8. Belmore, K.A.; Vanderpool, R.A.; Tsai, J. Cherng.; Khan, M.A.; Nicholas, K.M. Transition-Metal-Mediated Photochemical Disproportionation of Carbon Dioxide. *J. Am. Chem. Soc.* **1988**, *110*, 2004–2005. [CrossRef]
9. Matt, B.; Moussa, J.; Chamoreau, L.-M.; Afonso, C.; Proust, A.; Amouri, H.; Izzet, G. Elegant Approach to the Synthesis of a Unique Heteroleptic Cyclometalated Iridium(III)-Polyoxometalate Conjugate. *Organometallics* **2012**, *31*, 35–38. [CrossRef]
10. Zhou, X.; Yang, J.; Li, C. Theoretical Study of Structure, Stability, and the Hydrolysis Reactions of Small Iridium Oxide Nanoclusters. *J. Phys. Chem. A* **2012**, *116*, 9985–9995. [CrossRef]
11. Liu, R.; Dandu, N.; Chen, J.; Li, Y.; Li, Z.; Liu, S.; Wang, C.; Kilina, S.; Kohler, B.; Sun, W. Influence of Different Diimine (N ^ N) Ligands on the Photophysics and Reverse Saturable Absorption of Heteroleptic Cationic Iridium(III) Complexes Bearing Cyclometalating 2-{3-[7-(Benzothiazol-2-Yl)Fluoren-2-Yl]Phenyl}pyridine (C ^ N) Ligands. *J. Phys. Chem. C* **2014**, *118*, 23233–23246. [CrossRef]
12. Yao, C.; Tian, Z.; Jin, D.; Zhao, F.; Sun, Y.; Yang, X.; Zhou, G.; Wong, W.-Y. Platinum(II) Acetylide Complexes with Star- and V-Shaped Configurations Possessing Good Trade-off between Optical Transparency and Optical Power Limiting Performance. *J. Mater. Chem. C* **2017**, *5*, 11672–11682. [CrossRef]
13. Liu, R.; Zhu, S.; Lu, J.; Shi, H.; Zhu, H. Pt(II) Diimine Complexes Bearing Difluoro-Boron-Dipyrromethene Acetylide Ligands: Synthesis, Photophysics, Aggregation Included Emission and Optical Power Limiting Properties. *Dyes Pigments* **2017**, *147*, 291–299. [CrossRef]
14. You, Y.; Nam, W. Photofunctional Triplet Excited States of Cyclometalated Ir(Iii) Complexes: Beyond Electroluminescence. *Chem. Soc. Rev.* **2012**, *41*, 7061. [CrossRef]
15. Li, Y.; Dandu, N.; Liu, R.; Hu, L.; Kilina, S.; Sun, W. Nonlinear Absorbing Cationic Iridium(III) Complexes Bearing Benzothiazolylfluorene Motif on the Bipyridine (N∧N) Ligand: Synthesis, Photophysics and Reverse Saturable Absorption. *ACS Appl. Mater. Interfaces* **2013**, *5*, 6556–6570. [CrossRef]
16. Hirata, S.; Totani, K.; Yamashita, T.; Adachi, C.; Vacha, M. Large Reverse Saturable Absorption under Weak Continuous Incoherent Light. *Nat. Mater.* **2014**, *13*, 938–946. [CrossRef]
17. Dini, D.; Calvete, M.J.F.; Hanack, M. Nonlinear Optical Materials for the Smart Filtering of Optical Radiation. *Chem. Rev.* **2016**, *116*, 13043–13233. [CrossRef]
18. Yuan, G.-J.; Shao, D.-S.; Hu, B.-W.; Liu, W.-L.; Ren, X.-M. A Rotorlike Supramolecular Assembly, {[K(18-Crown-6)]PbI $_3$ } $_\infty$, with a Reversible Breaking-Symmetry Phase Transition near Room Temperature. *Inorg. Chem.* **2020**, *59*, 980–983. [CrossRef]
19. Tang, M.; Zhu, S.; Liu, R.; Wang, J.; Zhang, Z.; Zhu, H. Synthesis, Characterization and Optical Properties of Novel Ir(III) Complexes Bearing N-Heterocycle Substituents. *J. Organomet. Chem.* **2019**, *880*, 363–367. [CrossRef]

20. Lu, J.; Pan, Q.; Zhu, S.; Liu, R.; Zhu, H. Ligand-Mediated Photophysics Adjustability in Bis-Tridentate Ir(III) Complexes and Their Application in Efficient Optical Limiting Materials. *Inorg. Chem.* **2021**, *60*, 12835–12846. [CrossRef]
21. Liu, B.; Jabed, M.A.; Kilina, S.; Sun, W. Synthesis, Photophysics, and Reverse Saturable Absorption of *Trans* -Bis-Cyclometalated Iridium (III) Complexes (C^N^C)Ir(R-Tpy) $^{+}$ (Tpy = 2,2′:6′,2″-Terpyridine) with Broadband Excited-State Absorption. *Inorg. Chem.* **2020**, *59*, 8532–8542. [CrossRef] [PubMed]
22. Kuei, C.-Y.; Liu, S.-H.; Chou, P.-T.; Lee, G.-H.; Chi, Y. Room Temperature Blue Phosphorescence: A Combined Experimental and Theoretical Study on the Bis-Tridentate Ir(III) Metal Complexes. *Dalton Trans.* **2016**, *45*, 15364–15373. [CrossRef] [PubMed]
23. Whittle, V.L.; Williams, J.A.G. A New Class of Iridium Complexes Suitable for Stepwise Incorporation into Linear Assemblies: Synthesis, Electrochemistry, and Luminescence. *Inorg. Chem.* **2008**, *47*, 6596–6607. [CrossRef] [PubMed]
24. Kuei, C.-Y.; Tsai, W.-L.; Tong, B.; Jiao, M.; Lee, W.-K.; Chi, Y.; Wu, C.-C.; Liu, S.-H.; Lee, G.-H.; Chou, P.-T. Bis-Tridentate Ir(III) Complexes with Nearly Unitary RGB Phosphorescence and Organic Light-Emitting Diodes with External Quantum Efficiency Exceeding 31%. *Adv. Mater.* **2016**, *28*, 2795–2800. [CrossRef] [PubMed]
25. Gildea, L.F.; Batsanov, A.S.; Williams, J.A.G. Bright Orange/Red-Emitting Rhodium (Iii) and Iridium(Iii) Complexes: Tridentate N^C^N-Cyclometallating Ligands Lead to High Luminescence Efficiencies. *Dalton Trans.* **2013**, *42*, 10388. [CrossRef]
26. Guo, F.; Sun, W.; Liu, Y.; Schanze, K. Synthesis, Photophysics, and Optical Limiting of Platinum (II) 4′-Tolylterpyridyl Arylacetylide Complexes. *Inorg. Chem.* **2005**, *44*, 4055–4065. [CrossRef]
27. Shao, P.; Li, Y.; Sun, W. Cyclometalated Platinum (II) Complex with Strong and Broadband Nonlinear Optical Response. *J. Phys. Chem. A* **2008**, *112*, 1172–1179. [CrossRef]
28. Yi, J.; Zhang, B.; Shao, P.; Li, Y.; Sun, W. Synthesis and Photophysics of Platinum (II) 6-Phenyl-4-(9,9-Dihexylfluoren-2-Yl)-2,2′-Bipyridine Complexes with Phenothiazinyl Acetylide Ligand. *J. Phys. Chem. A* **2010**, *114*, 7055–7062. [CrossRef]
29. Wu, S.-H.; Ling, J.-W.; Lai, S.-H.; Huang, M.-J.; Cheng, C.H.; Chen, I.-C. Dynamics of the Excited States of [Ir(Ppy) $_2$ Bpy] $^{+}$ with Triple Phosphorescence. *J. Phys. Chem. A* **2010**, *114*, 10339–10344. [CrossRef]
30. Zhao, Q.; Liu, S.; Shi, M.; Wang, C.; Yu, M.; Li, L.; Li, F.; Yi, T.; Huang, C. Series of New Cationic Iridium(III) Complexes with Tunable Emission Wavelength and Excited State Properties: Structures, Theoretical Calculations, and Photophysical and Electrochemical Properties. *Inorg. Chem.* **2006**, *45*, 6152–6160. [CrossRef]
31. Zhu, Z.-L.; Chen, W.-C.; Ni, S.-F.; Yan, J.; Wang, S.F.; Fu, L.-W.; Tsai, H.-Y.; Chi, Y.; Lee, C.-S. Constructing Deep-Blue Bis-Tridentate Ir(III) Phosphors with Fluorene-Based Dianionic Chelates. *J. Mater. Chem. C* **2021**, *9*, 1318–1325. [CrossRef]
32. Tai, W.-S.; Gnanasekaran, P.; Chen, Y.-Y.; Hung, W.-Y.; Zhou, X.; Chou, T.-C.; Lee, G.-H.; Chou, P.-T.; You, C.; Chi, Y. Rational Tuning of Bis-Tridentate Ir(III) Phosphors to Deep-Blue with High Efficiency and Sub-Microsecond Lifetime. *ACS Appl. Mater. Interfaces* **2021**, *13*, 15437–15447. [CrossRef]
33. Zhu, S.; Pan, Q.; Li, Y.; Liu, W.; Liu, R.; Zhu, H. Fluorene-Decorated Ir (III) Complexes: Synthesis, Photophysics and Tunable Triplet Excited State Properties in Aggregation. *Dalton Trans.* **2022**, *51*, 13322–13330. [CrossRef]
34. Liu, J.-Q.; Luo, Z.-D.; Pan, Y.; Kumar Singh, A.; Trivedi, M.; Kumar, A. Recent Developments in Luminescent Coordination Polymers: Designing Strategies, Sensing Application and Theoretical Evidences. *Coord. Chem. Rev.* **2020**, *406*, 213145. [CrossRef]
35. Zhou, S.; Lu, L.; Liu, D.; Wang, J.; Sakiyama, H.; Muddassir, M.; Nezamzadeh-Ejhieh, A.; Liu, J. Series of Highly Stable Cd (ii)-Based MOFs as Sensitive and Selective Sensors for Detection of Nitrofuran Antibiotic. *CrystEngComm* **2021**, *23*, 8043–8052. [CrossRef]
36. Büldt, L.A.; Guo, X.; Vogel, R.; Prescimone, A.; Wenger, O.S. A Tris(Diisocyanide)Chromium(0) Complex Is a Luminescent Analog of Fe(2,2′-Bipyridine)$_3^{2+}$. *J. Am. Chem. Soc.* **2017**, *139*, 985–992. [CrossRef]
37. Lu, T.; Wang, C.; Lystrom, L.; Pei, C.; Kilina, S.; Sun, W. Effects of Extending the π-Conjugation of the Acetylide Ligand on the Photophysics and Reverse Saturable Absorption of Pt(ii) Bipyridine Bisacetylide Complexes. *Phys. Chem. Chem. Phys.* **2016**, *18*, 28674–28687. [CrossRef]
38. Hongbing, Z.; Wenzhe, C.; Minquan, W.; Chunlin, Z. Optical Limiting Effects of Multi-Walled Carbon Nanotubes Suspension and Silica Xerogel Composite. *Chem. Phys. Lett.* **2003**, *382*, 313–317. [CrossRef]

Disclaimer/Publisher's Note: The statements, opinions and data contained in all publications are solely those of the individual author(s) and contributor(s) and not of MDPI and/or the editor(s). MDPI and/or the editor(s) disclaim responsibility for any injury to people or property resulting from any ideas, methods, instructions or products referred to in the content.